processes

MDPI

Article

Study on the Influence of Industrial Coke Oven Size on the Quality of Metallurgical Coke

Liangyuan Hao [1,2], Jianliang Zhang [1,3,*], Huan Cheng [4,5,*], Luying Xiao [6], Fei Liao [4] and Wenjia Hu [4]

[1] School of Metallurgical and Ecological Engineering, University of Science and Technology Beijing, Beijing 100083, China; b20200099@xs.ustb.edu.cn
[2] Strategic Research Institute, HBIS Group Co., Ltd., Shijiazhuang 050023, China
[3] State Key Laboratory of Advanced Metallurgy, University of Science and Technology Beijing, Beijing 100083, China
[4] College of Chemical Engineering, North China University of Science and Technology, Tangshan 063210, China; liaofeiwower@163.com (F.L.); kongzhuling@163.com (W.H.)
[5] Jiangsu Yonggang Group Co., Ltd., Suzhou 215628, China
[6] College of Science, North China University of Science and Technology, Tangshan 063210, China; luyingxiao20201010@163.com
* Correspondence: zhang.jianliang@hotmail.com (J.Z.); chenghuan@ncst.edu.cn (H.C.)

Abstract: The large-scale coke oven is a developing trend in coking technology, and the influence of the industrial coke oven size on the quality of metallurgical coke needs to be revealed. Under the same raw coals and blending ratios, metallurgical cokes were obtained from top-loading coke ovens with carbonization chamber heights of 6 and 7 m, respectively. The macroscopic quality and microstructure of the refined metallurgical cokes were comprehensively tested. The results showed that the conventional cold and thermal strength indexes of Coke-7m were better than those of Coke-6m. The comprehensive thermal strength at multiple temperatures further showed that the thermal strength advantage of Coke-7m was mainly manifested at low temperatures (1050 and 1100 °C) or a high temperature (1300 °C), where the solution-loss reaction mode of coke tended to be the "uniform reaction model" or "unreacted core model". At medium temperatures, the solution-loss reaction mode tended to be the "gradient reaction model", which had a greater destructive effect on the thermal strength of coke. At this time, the thermal strengths of the two cokes were close. Microstructure characterization revealed that industrial coke oven size mainly affected the carbon structure of coke but had little effect on pore structure. The advantage of Coke-7m regarding carbon structure is an important reason for its superior macroscopic quality compared to Coke-6m.

Keywords: metallurgical coke; coke oven; thermal strength; carbon structure; pore structure

check for updates

Citation: Hao, L.; Zhang, J.; Cheng, H.; Xiao, L.; Liao, F.; Hu, W. Study on the Influence of Industrial Coke Oven Size on the Quality of Metallurgical Coke. *Processes* **2024**, *12*, 1637. https://doi.org/10.3390/pr12081637

Academic Editors: Yueliang Liu, Shaoqi Kong, Chuang Wen and Raymond Cecil Everson

Received: 11 July 2024
Revised: 27 July 2024
Accepted: 30 July 2024
Published: 3 August 2024

Copyright: © 2024 by the authors. Licensee MDPI, Basel, Switzerland. This article is an open access article distributed under the terms and conditions of the Creative Commons Attribution (CC BY) license (https://creativecommons.org/licenses/by/4.0/).

1. Introduction

China is a major coke-producing country, accounting for about more than 60% of the world's total output [1]. In 2021, China's coke production reached 464 million tons [2]. This high coke production is suitable for meeting the needs of its large steel industry. Coke mainly plays the role of heating, reduction, carburizing, and acting as the skeleton for the charge column in the blast furnace [3]. Among them, the role of charge-column skeleton is particularly important and as of yet cannot be replaced by other technologies. With the development of larger blast furnaces, higher requirements were put forward for the quality of metallurgical coke. At present, proximate analysis [4], sulfur content [5], mechanical strength [6], and thermal properties [7] are mainly used to evaluate coke quality in China.

Among the methods for evaluating coke quality, thermal properties have traditionally been highly valued by coke makers because they reflect the solution loss and degradation behavior of coke in the blast furnace [8]. Currently, the mainstream method for evaluating coke thermal properties is the NSC method proposed by Nippon Steel Corporation in the

1970s. In this method, coke samples with a certain particle size (19~21 mm) and mass (200 g) are reacted with pure CO_2 gas at 1100 °C for 2 h to determine the reactivity CRI and strength after reaction CSR indexes of coke [9].

Although the NSC method has played an important role in evaluating coke quality, some scholars have questioned its scientific validity, mainly focusing on the following points: (1) a single 1100 °C test temperature is not sufficient to reflect the solution-loss behavior of coke occurring in the temperature range of 900~1300 °C near the soft melting zone of a blast furnace [10]; (2) the fixed reaction time of 2 h causes the solution loss of some cokes to not be in accordance with their real values in the blast furnace (around 20%~30%) [11]; (3) the pure CO_2 atmosphere is not exactly consistent with the actual atmospheric environment in the blast furnace [12]; and (4) the effect of alkali metal catalysis is not reflected [13].

Essentially, coke is a porous and brittle carbonaceous material, and its macroscopic properties mainly depend on its microstructure (carbon structure and pore structure). In terms of carbon structure, the optical texture structure measured by optical microscopy indicated that the degree of anisotropy of each optical texture type had an important effect on the reactivity and strength after the reaction of coke [12]. The microcrystalline structure obtained by X-ray diffraction (XRD) showed that the larger the size of microcrystalline units, the denser the structure, and the better the thermal performance of coke [14]. In terms of pore structure, some scholars have pointed out that coke strength was determined by the pore structure in the matrix [15]. Guo et al. [16] suggested that micron-sized pores in the range of 60~120 μm were the main diffusion channels for the gas–solid reaction and had a positive effect on the reactivity of coke. It has also been shown that the nano-pore structure affected the solution-loss reaction behavior of coke and therefore was closely related to the thermal properties of coke [17].

After decades of development in China's coking industry, different volume types of coke ovens with coking chamber heights of 4.3, 5.5, 6, 7, and 7.63 m have been built successively. Large-scale coke ovens are the development trend of coking technology [18]. At present, coke ovens with coking chamber heights of 6 and 7 m are the mainstream oven types in China. However, the differences in coke quality from various sizes of coke ovens have rarely been reported. This is mainly because coal-blending proportions differed between enterprises with different oven types. Therefore, the results could not be accurately compared. Additionally, one enterprise would rarely simultaneously have coke ovens of different sizes. This research enterprise has both 42-hole top-loading coke ovens with coking chamber heights of 6 and 7 m, respectively. The single-hole coal-loading capacity of the 6 m coke oven is 28 t (dry basis), and that of the 7 m coke oven is 36 t (dry basis). The annual output of the 6 m coke oven is about 400,000 tons, and that of the 7 m coke oven is about 500,000 tons. The characteristic of our research is to use the same raw coal and proportion of coke in 6 and 7 m coke ovens, respectively, and comprehensively test the quality of the refined coke, thereby elucidating the influence of industrial coke oven size on the quality of metallurgical coke.

2. Materials and Methods

2.1. Blending Coal and Coking Test

The raw material used in the coking was blending coal. Blending coal refers to the coal material that was mixed using a variety of single coals according to the principle of economic rationality. Single coal types used in the coking included gas coal, 1/3 coking coal, fat coal, coking coal, lean coal, etc. The ratios of each type of coal in the coal blend were determined according to the quality of coke produced to reach a certain level, as shown in Table 1.

Table 1. The ratios of each type of coal in the coal blend.

Coal Type	Ratio (%)	Source
Gas coal	9	Shandong, China
1/3 coking coal	8	Henan, China
Fat coal	25	Shanxi, China
Coking coal	44	Shanxi, China
Lean coal	14	Shanxi, China
Total	100	

Before loading it into the coke ovens, the basic properties of the blending coal were tested, including total moisture content M_t, ash content A_d, volatile matter V_{daf}, carbon content FC_{ad}, sulfur content $S_{t,d}$, average maximum vitrinite reflectance R_{max}, and thermoplastic indexes (caking index G and plastic layer index Y). The results are shown in Table 2.

Table 2. The basic property indexes of blending coal.

Name	Proximate Analysis, wt %				$S_{t,d}$ (%)	R_{max} (%)	Thermoplastic Indexes		Bulk Density (t/m^3)	Fineness (%)
	M_t	A_d	V_{daf}	FC_{ad}			G	Y (mm)		
Blending coal	11.64	9.68	26.60	64.40	0.90	1.32	71.53	16.75	0.75	70

The blending coal was loaded into the coke ovens with coking chamber heights of 6 and 7 m, respectively, for coking. The bulk density was controlled at about 0.75 t/m^3. The fineness was controlled at 70% (see Table 2). The center temperature of the coke cake was controlled at around 1000 °C, and the coking time was 19 h. After the coking process was complete, the coke was pushed out of the coking chamber by a coke pusher, and the coke was cooled by dry quenching.

2.2. Determination of Coke Conventional Quality Indexes

To comprehensively evaluate the quality difference of metallurgical cokes refined by coke ovens with different coking chamber heights of 6 and 7 m, the conventional quality indexes such as proximate analysis, sulfur content, mechanical strength, and thermal properties of the cokes were determined. The proximate analysis indexes (moisture M_{ad}, ash A_d, and volatile matter V_{daf}) were determined in accordance with the Chinese national standard GB/T 2001-2013. The sulfur content $S_{t,d}$ was determined according to the Chinese national standard GB/T 2286-2017. The mechanical strength indicators (crushing strength M_{40} and abrasion resistance M_{10}) were determined in accordance with the Chinese national standard GB/T 2006-2008. The thermal property indexes (reactivity CRI and strength after reaction CSR) were determined according to the Chinese national standard GB/T 4000-2017. It should be noted that the determination method of coke's thermal properties as specified in the Chinese national standard GB/T 4000-2017 is an improved NSC method, and the particle size of the tested coke samples is 23~25 mm.

2.3. Determination of Coke Thermal Strength at Multiple Temperatures

In view of the fact that the conventional NSC method may not be able to fully reflect the solution-loss and deterioration behavior of coke in a blast furnace, a self-developed large-scale supporting thermal balance device was used in this study to determine the thermal strength values of coke at multiple temperatures. The schematic diagram of the device is shown in Figure 1. The device is mainly composed of a high-temperature resistance corundum reactor, precision electronic balance, electric heating furnace, gas supply system, and comprehensive control cabinet. The selection of reaction temperatures mainly considered simulation of the temperature range where the solution-loss reaction of coke occurs near the soft melting zone in the blast furnace.

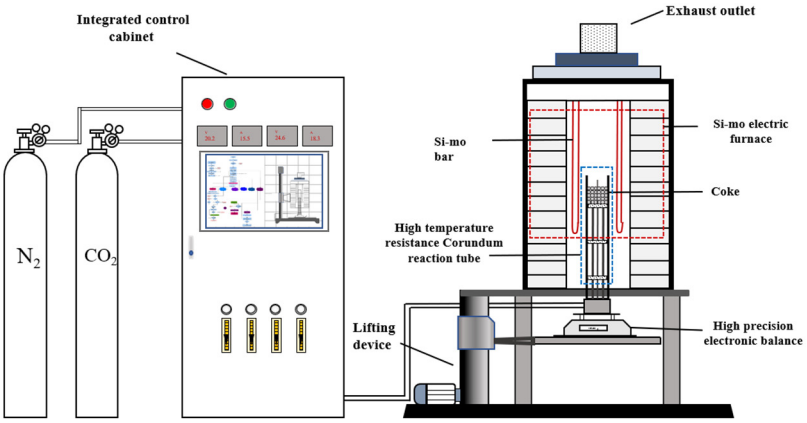


Figure 1. Schematic diagram of the large-scale supporting thermal balance device.

The specific experimental steps were as follows. Metallurgical cokes refined from 6 and 7 m coke ovens were selected, and six sets of coke samples with particle size of 23~25 mm and mass of 200 ± 0.5 g were prepared, respectively, for both of the two cokes. Thermal strength tests of coke at different target temperatures were carried out six times. The prepared coke samples were placed into the reactor and heated up to the specified target temperature under the protection of N_2 atmosphere. The six target temperatures selected for this study were 1050, 1100, 1150, 1200, 1250, and 1300 °C. When the temperature of coke samples reached the specified target temperature, N_2 was switched to CO_2 (flow rate was 5 L/min). Then, the coke began to undergo a solution-loss reaction. When the coke solution-loss degree reached 25%, the experiment was stopped, and the CO_2 was switched back to N_2 protection. When the coke samples were cooled to room temperature, the samples were taken out, and their thermal strength value, CSR_{25} (%), was determined by the I-drum test. It should be emphasized that the I-drum test method used in the multi-temperature thermal strength test of coke was exactly the same as the improved NSC method specified in the Chinese national standard GB/T 4000-2017.

2.4. Characterization of Coke Microstructure

The microstructure of coke includes carbon structure and pore structure, both of which were characterized using various techniques.

2.4.1. Carbon Structure

The carbon structure of coke was characterized by optical microscopy and X-ray diffraction (XRD).

According to the Chinese ferrous metallurgy industry standard YB/T 077-2017, the optical texture structure of coke was measured by a German Zeiss MY-6000 (German) polarizing microscope, and the measured optical textures included isotropic texture, fine mosaic texture, medium mosaic texture, coarse mosaic texture, incompletely fibrous texture, completely fibrous texture, leaflet texture, and fusinite and fragmental texture.

The coke microcrystalline structure was determined by the German BRUKER D8 ADVANCE X-ray (German) diffractometer with Cu target radiation, line tube voltage of 40 kV, line tube current of 40 mA, scanning speed of 2°/min, step size of 0.002°, and scanning range of 5~95°. Based on the X-ray diffraction pattern of coke, the microcrystalline structure parameters, such as the microcrystalline stacking height L_c (nm), diameter L_a (nm), and interlayer spacing d_{002} (nm) [19] can be calculated by using the Scherrer and Bragg equations. The calculation formulas are shown in Equations (1)–(3).

$$L_c = \frac{k_2 \lambda}{\beta_{002} cos\theta_{002}} \quad (1)$$

$$L_a = \frac{k_1 \lambda}{\beta_{100} cos\theta_{100}} \quad (2)$$

$$d_{002} = \frac{\lambda}{2sin\theta_{002}} \quad (3)$$

where λ is the wavelength of X-ray radiation (0.15406 nm), θ_{002} is the diffraction angle corresponding to the 002 peak (°), θ_{100} is the diffraction angle corresponding to the 100 peak (°), β_{002} is the full width of half-maximum intensity of the 002 peak (nm), β_{100} is the full width of half-maximum intensity of the 100 peak (nm), k_1 and k_2 are constants, k_1 = 1.84, and k_2 = 0.89.

2.4.2. Pore Structure

The micro-pores and nano-pores of coke were characterized, respectively.

Characterization of micro-pore structure. Representative coke blocks were collected, and cubic blocks with sides of 2~3 cm were cut out to be tested. One side of the coke block was selected and sandpapered gradually with sandpaper of different fineness grades until a smooth qualified surface was obtained. The smooth surface was polished with polishing solution. Finally, the coke samples were dried at 175 °C for 2 h. The MAC Smart Scope 2000 series automatic intelligent pore structure analyzer was used to detect the micro-pore structure of coke. The measurement parameters included average pore size (APS, μm), average pore-wall thickness (APWT, μm), porosity (P, %), and pore size distribution (PSD).

Characterization of nano-pore structure. The coke samples were crushed to 1~3 mm and then dried at 120 °C for 2 h. The BSD 3H-2000PM1 low-temperature N_2 adsorption instrument was used to detect the nano-pore structure of coke. The mass of tested coke samples was around 1000 mg, the degassing temperature was 200 °C, and the degassing time was 480 min. The parameters measured included specific surface area S (m^2/g), pore volume V (mm^3/g), average pore size $\overline{r}$ (nm), and pore size distribution (PSD).

3. Results and Discussion

3.1. Influence on the Conventional Coke Quality Indexes

The proximate analysis and sulfur content indexes of metallurgical cokes refined from 6 and 7 m top-loading coke ovens are shown in Table 3. The moisture contents M_{ad}s of the two cokes were 0.41% and 0.37%, respectively. Both were at a low level, which was related to the use of dry quenching. Due to the use of the same raw coals, the ash content A_ds and sulfur content $S_{t,d}$s of the two cokes were similar, with values of 12.28%, 12.25% and 0.84%, 0.82%, respectively. The volatile matter index V_{daf} showed that the volatile matter contents of the two cokes were both between 1%~2%, indicating that both of them were mature.

Table 3. Proximate analysis and sulfur content of coke samples.

Coke Sample	Proximate Analysis, wt %			$S_{t,d}$ (%)
	M_{ad}	A_d	V_{daf}	
Coke-6m	0.41	12.28	1.19	0.84
Coke-7m	0.37	12.25	1.14	0.82

The mechanical strength indicators of the two cokes are shown in Table 4. The principle for detecting and calculating the mechanical strength M_{40} and M_{10} is as follows: a 15 kg coke sample with a particle size greater than 60 mm was loaded into a drum with a diameter and length of 1000 mm and rotated at a speed of 25 r/min for 4 min. Then, the coke inside the drum was taken out and sieved. The percentage of coke particles larger than 40 mm in total mass is defined as the compressive strength index M_{40}, while the percentage of coke particles smaller than 10mm in total mass is defined as the wear resistance index M_{10}. The higher M_{40} value and the lower M_{10} value means the better mechanical properties of coke in the cold state. The test of coke mechanical strength index was repeated three times. If

the repeatability of the results of the three experiments was within 1%, the results were considered reasonable. Finally, the average value of the three experimental results was taken as the index value. It can be seen that the crushing strength M_{40} of Coke-7m was slightly higher than that of Coke-6m, which were 88.90% and 87.08%, respectively, with a difference of +1.82%. The abrasion resistance M_{10} showed that the M_{10} value of Coke-7m was lower than that of Coke-6m, which were 5.20% and 6.41% respectively, with a difference of −1.21%. Overall, the cold mechanical performance of Coke-7m is better than that of Coke-6m.

Table 4. Mechanical strength index of coke samples.

Coke Sample	M_{40} (%)	M_{10} (%)
Coke-6m	87.08	6.41
Coke-7m	88.90	5.20

The thermal property indexes (reactivity CRI and strength after reaction CSR) of the two cokes detected by the improved NSC method are shown in Table 5. The test of coke conventional thermal property indexes was repeated three times. If the repeatability of the results of the three experiments was within 1%, the results were considered reasonable. Finally, the average value of the three experimental results was taken as the index value. The reactivity indexes' CRIs of Coke-6m and Coke-7m were close, with 23.48% and 22.63%, respectively. The CRI value of Coke-7m was slightly lower than that of Coke-6m, with the absolute value of the difference being within 1%. Compared with the reactivity CRI index, the difference between the strength after the reaction indexes' CSRs of the two cokes was larger. The CSR values of Coke-6m and Coke-7m were 66.03% and 67.90%, respectively. The strength after reaction of Coke-7m was higher than that of Coke-6m, with a difference of nearly 2%. It can be seen that the influence of coke oven size on the strength after reaction is greater than on the reactivity. Overall, the thermal properties of Coke-7m are better than those of Coke-6m.

Table 5. Thermal property indexes of coke samples measured by the conventional NSC method.

Coke Sample	CRI (%)	CSR (%)
Coke-6m	23.48	66.03
Coke-7m	22.63	67.90

3.2. Influence on the Coke Thermal Strength Indexes at Multiple Temperatures

The traditional test method of coke thermal properties only investigated the thermal properties of coke at one temperature of 1100 °C, which may not fully reflect the real thermal performance difference between the two cokes in a blast furnace. Therefore, in this study, the self-developed coke thermal strength test at multiple temperatures was added on the basis of the traditional NSC method, and the results are shown in Table 6. The CSR_{25} index obtained at multiple temperatures (1050~1300 °C) can comprehensively reflect the change of thermal strength of coke in the soft melting zone of the blast furnace and provide more information about thermal properties. Therefore, this index can play an important role in the comprehensive analysis of the difference in thermal performance between Coke-6m and Coke-7m. The repeatability of the CSR_{25} index was consistent with the traditional thermal property index (CSR).

Table 6. The coke thermal strength test results at multi-temperatures.

Coke Sample	CSR_{25} (%)					
	1050 °C	1100 °C	1150 °C	1200 °C	1250 °C	1300 °C
Coke-6m	66.17	64.01	57.76	59.22	61.57	63.37
Coke-7m	68.86	65.53	58.11	59.62	61.65	64.56

The thermal strength values of Coke-6m at 1050~1300 °C were 57.76%~66.17%, with a maximum difference of 8.41%. The thermal strength values of Coke-7m at 1050~1300 °C were 58.11%~68.86%, with a maximum difference of 10.75%. The test results of the two cokes show that there are significant differences in the measured thermal strength values with different reaction temperatures.

Based on the traditional NSC test temperature of 1100 °C, the differences between the thermal strength values measured at other reaction temperatures and this temperature were analyzed. When the reaction temperature was lower, at 1050 °C, the measured thermal strength values were higher, 66.17% and 68.86% for Coke-6m and Coke-7m, respectively (see Table 6), which were 2.16% and 3.33% higher than their thermal strength values measured at 1100 °C (see Table 7). However, when the reaction temperature was increased to 1150 °C, the thermal strength of both of the two cokes decreased significantly. The thermal strength values of Coke-6m and Coke-7m were only 57.76% and 58.11%, respectively (see Table 6), which were 6.25% and 7.42% lower than their thermal strength values measured at 1100 °C (see Table 7). The thermal strength values measured at 1200 °C, 1250 °C, and 1300 °C were still generally lower than those at 1100 °C, but the difference showed a gradual decrease with the increase in reaction temperature. From the above analysis, it can be seen that the reaction temperature has a significant impact on the thermal strength of coke. The traditional NSC method, which simply measures the thermal strength of coke at one temperature of 1100 °C, reflects limited information.

Table 7. The difference in coke thermal strength at multi-temperatures based on the value of 1100 °C.

Coke Sample	ΔCSR_{25} (%)					
	1050 °C	1100 °C	1150 °C	1200 °C	1250 °C	1300 °C
Coke-6m	+2.16	0	−6.25	−4.79	−2.44	−0.64
Coke-7m	+3.33	0	−7.42	−5.91	−3.88	−0.97

The variation of the thermal strength CSR_{25} measured at multiple temperatures with the reaction temperature T for the two cokes is shown in Figure 2. With the increase in reaction temperature T, the thermal strength values of both of the two cokes show a changing law of first decreasing and then increasing. This trend may be related to the fact that coke has different solution-loss modes at different reaction temperatures.

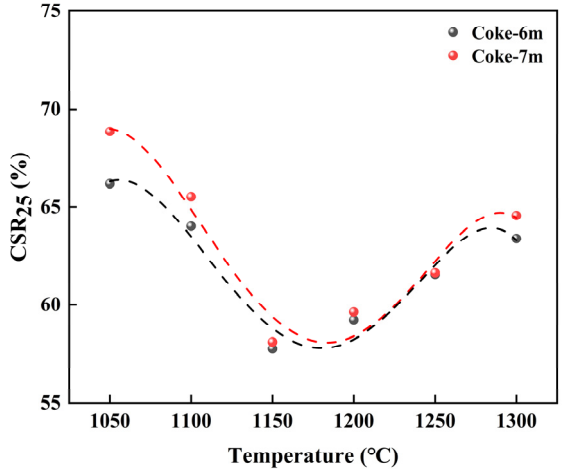


Figure 2. Variation of coke thermal strength CSR_{25} at multi-temperatures with reaction temperature T.

The solution-loss reaction of coke with CO_2 gas molecules is a classical solid–gas two-phase reaction. Since coke is a porous carbonaceous material, the reaction may be affected by two factors: the chemical reaction rate of carbon matrix and the diffusion resistance in the pore channels [20]. At low temperatures, the solution-loss mode of coke and CO_2 tends

to be the "uniform reaction model"; that is, at low temperatures, the chemical reaction rate is relatively slow, which is the limiting link of the whole process. CO_2 gas molecules can smoothly penetrate the coke. Since the reaction amount of each part of the coke is relatively uniform, the overall thermal strength is higher. With the increase in reaction temperature, the chemical reaction rate of the carbon matrix accelerates, and the internal diffusion resistance generated by the pores inside the coke competes effectively with the chemical reaction rate of the carbon matrix, so that the coke solution-loss reaction mode is gradually transformed into a "gradient reaction model". This mode is more serious regarding the destruction of coke strength, so that the thermal strength value is relatively low. With the further increase in reaction temperature, the internal diffusion resistance gradually becomes the limiting link, and the solution-loss reaction between the coke and CO_2 gas molecules is mainly carried out on the surface section of coke. That is, the solution-loss reaction mode of coke tends to be an "unreacted core model", which protects the "core" of coke to some extent. Therefore, the thermal strength value of coke increases again [11]. In general, the thermal strength values of the two cokes at low temperatures (1050 and 1100 °C) were higher than those at medium and high temperatures (1150~1300 °C), which may be related to the increasing influence of thermal stress on the thermal strength of coke at elevated temperatures [21].

A detailed comparison was conducted between the thermal strength values of Coke-6m and Coke-7m at multiple temperatures. The results show that the thermal strength value of Coke-7m at each temperature is generally higher than that of Coke-6m. This indicates that the comprehensive thermal performance of Coke-7m is better than that of Coke-6m. However, there is a certain distinction in the difference between the thermal strength values of the two cokes under different temperature conditions. The difference between the thermal strength values of the two cokes at multiple temperatures and its variation with the reaction temperature T are shown in Figure 3. At low temperatures (1050 and 1100 °C), the thermal strength value of Coke-7m is higher than that of Coke-6m (+2.69% at 1050 °C and +1.52% at 1100 °C). However, under the middle three temperature conditions (1150, 1200, and 1250 °C), the thermal strength values of the two cokes are close, and the thermal strength value of Coke-7m is only slightly higher than that of Coke-6m. But when the reaction temperature is further increased to 1300 °C, the difference between the thermal strength values of the two cokes increases further, and the thermal strength value of Coke-7m is +1.19% higher than that of Coke-6m. In general, the difference between the thermal strength values of the two cokes at multiple temperatures shows a high-low-high "U" shaped trend with the increase in reaction temperature T.

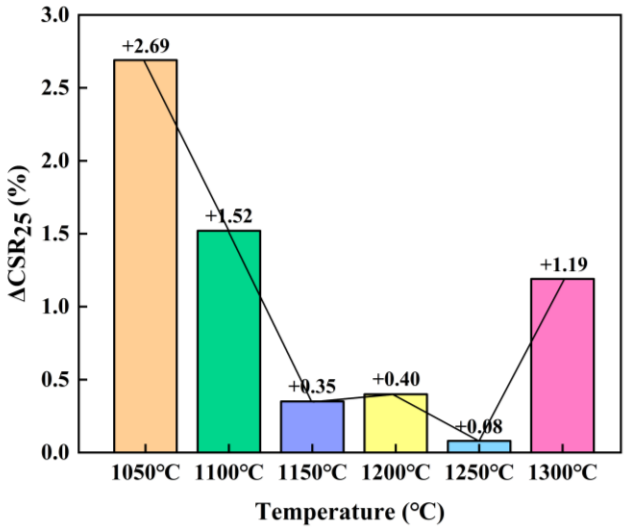


Figure 3. The difference between the thermal strength values of the two cokes under multi-temperature conditions as well as their variation with the reaction temperature T.

Based on the different solution-loss reaction modes of coke at different reaction temperatures, it can be seen that at low or high temperatures, the solution-loss reaction mode of coke tends to be the "uniform reaction model" or "unreacted core model", and the thermal strength of Coke-7m is obviously higher than that of Coke-6m. At intermediate temperatures, the solution-loss reaction mode tends to be the "gradient reaction model", and the thermal strengths of the two cokes are close. The common characteristic of the two cokes at this time is that the solution-loss reaction mode has a significant destructive effect on their thermal strength, and the thermal strength values of both of the two cokes are relatively low.

From the comprehensive comparative analysis of the macroscopic quality indexes of the two cokes, it can be found that the chemical compositions of the two cokes are similar, which may be related to the use of the same raw coals and blending ratios. The cold strength of Coke-7m is higher than that of Coke-6m. Similarly, both the traditional NSC thermal property index (CSR) and the newly proposed multi-temperature thermal strength index (CSR_{25}) show that the thermal performance of Coke-7m is better than that of Coke-6m. Large-capacity coke ovens have better macroscopic quality indexes of refined metallurgical coke because of the higher height of the coking chamber, higher bulk density of the loaded coal, more contact points between the thermal coal particles, and more liquid-phase and gas-phase products generated by the pyrolysis, which increases the swelling pressure of the coking process, facilitates the surface adhesion and interfacial reaction of coal particles, and the increases the uniformity of coke maturation [22].

It is well known that the macroscopic properties of coke mainly depend on its microstructure. In order to further elucidate the influence of different coke oven sizes on the quality of refined metallurgical coke, it is necessary to characterize the microstructures of the two cokes.

3.3. Influence on the Carbon Structure

The coke microstructure includes carbon structure and pore structure. For the carbon structure, the optical texture structure of the two cokes was characterized by optical microscopy, and the microcrystalline structure of the two cokes was characterized by X-ray diffraction.

3.3.1. Optical Texture

The optical texture structure parameters of the two cokes are shown in Table 8. The result is the average of the three coke samples. Comparing and analyzing the content of each optical texture in the two cokes, it can be seen that the contents of isotropic texture, fine mosaic texture, and medium mosaic texture are higher in Coke-6m, while the contents of coarse mosaic texture and fibrous texture are higher in Coke-7m, especially the coarse mosaic texture, which is 6.8% higher in Coke-7m than in Coke-6m. Fujita et al.'s results indicated that coarse mosaic and fibrous textures have strong resistance to mechanical stress and CO_2 erosion [23]. Therefore, the higher contents of coarse mosaic texture and fibrous texture in Coke-7m may be an important reason for its better macroscopic properties than Coke-6m.

Table 8. The optical texture components of coke samples.

Coke Sample	Content of Different Optical Textures (vol. %)							
	Isotropic Texture	Fine Mosaic Texture	Medium Mosaic Texture	Coarse Mosaic Texture	Incompletely Fibrous Texture	Completely Fibrous Texture	Leaflet Texture	Fusinite and Fragmental Texture
Coke-6m	2.9	12.7	56.0	2.7	0.0	0.0	2.0	23.7
Coke-7m	1.8	10.2	47.8	9.5	0.7	1.7	0.7	27.6

The optical anisotropy degree of each optical texture in coke is different, and the optical anisotropy index (OTI) can be obtained by assigning weights to them and summing

them up [24]. The weight values for the anisotropy degrees of different optical textures are shown in Table 9, and the OTIs calculated for the two cokes are compared in Figure 4. It can be found that the OTIs of the two cokes are very similar, indicating that the overall optical anisotropy degrees of the optical texture components in the two cokes are close.

Table 9. The anisotropic degree assignment of each optical texture type.

Optical Texture Type	Assignment
Isotropic texture	0.0
Fine mosaic texture	1.0
Medium mosaic texture	1.5
Coarse mosaic texture	2.0
Incompletely fibrous texture	2.5
Completely fibrous texture	3.0
Leaflet texture	4.0
Fusinite and fragmental texture	0.0

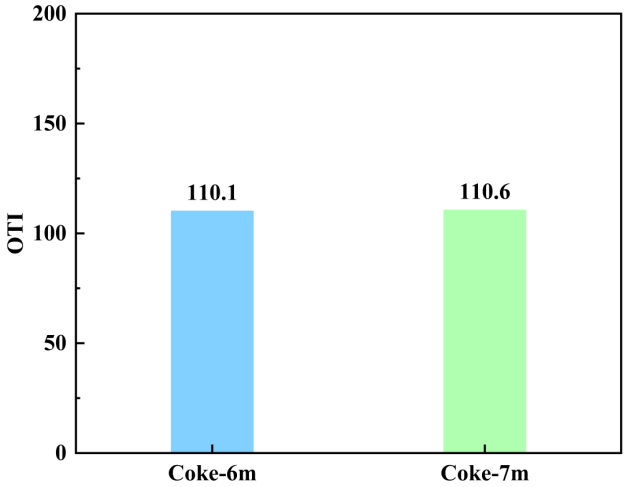


Figure 4. The optical anisotropy index (OTI) of coke samples.

Therefore, it can be inferred that the industrial coke oven size has little influence on the overall optical anisotropy degree of metallurgical coke optical texture, but it has a significant influence on the specific optical texture components. The higher contents of coarse mosaic texture and fibrous texture in metallurgical coke refined by large-capacity coke ovens may be an important reason for its better macroscopic performance.

3.3.2. Microcrystalline Structure

The XRD patterns of the two cokes are shown in Figure 5. It shows that there is a significant characteristic peak with a high peak value between 20 and 30° and a characteristic peak with a low peak value between 40 and 50°. The above two characteristic peaks reflect the microcrystalline structure of coke. Based on the nature of the characteristic peaks, the microcrystalline structure parameters of the two cokes can be calculated according to the Scherrer and Bragg equations, i.e., the microcrystalline stacking height L_c (nm), diameter L_a (nm), and interlayer spacing d_{002} (nm) [19]. The results are shown in Table 10.

Table 10. The microcrystalline structure parameters of coke samples.

Coke Sample	L_c (nm)	L_a (nm)	d_{002} (nm)
Coke-6m	1.78	4.82	0.3419
Coke-7m	1.90	4.99	0.3414

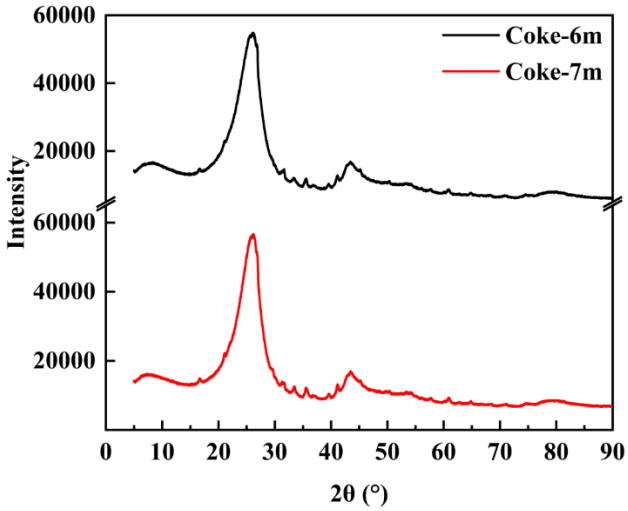


Figure 5. The XRD patterns of coke samples.

The microcrystalline stacking height L_c and diameter L_a of Coke-7m are both higher than those of Coke-6m, indicating that the microcrystalline size of Coke-7m is larger than that of Coke-6m. It can be seen from the interlayer spacing d_{002} that the interlayer spacing of Coke-7m is smaller than that of Coke-6m, indicating that the microcrystalline structure of Coke-7m is denser. Zheng et al.'s results showed that the large size and dense structure of microcrystalline coke are helpful in resisting mechanical stress and CO_2 erosion [25]. This may be an important reason why the macroscopic performance of Coke-7m is better than Coke-6m.

3.4. Influence on the Pore Structure

The pore structure of coke is relatively complex, and the size range is widely distributed, covering both micro-pores and nano-pores. The micro-pores of coke were characterized by optical microscopy, and the nano-pores were characterized by low-temperature N_2 adsorption.

3.4.1. Micro-Pore Structure

The micro-pore structure parameters of coke samples are shown in Table 11. The result is the average of the five coke samples. In general, the parameters of average pore size (APS), average pore-wall thickness (APWT), and porosity (P) of Coke-6m and Coke-7m were close, indicating that the micro-pore structure characteristics of the two cokes were similar. Specifically, the APS of Coke-7m was slightly smaller than that of Coke-6m, the APWT was slightly larger than that of Coke-6m, and the P was slightly lower than that of Coke-6m.

Table 11. Micro-pore structure parameters of coke samples.

Coke Sample	Average Pore Size APS (μm)	Average Pore-Wall Thickness APWT (μm)	Porosity P (%)
Coke-6m	87.31	59.30	60.66
Coke-7m	87.06	59.54	59.94

To further compare and analyze the micro-pore structure of coke samples, the pore size distributions of the two cokes were plotted, as shown in Figure 6. The pore size distribution curves of Coke-6m and Coke-7m almost overlap, further indicating that the micro-pore structures of the two cokes are very similar.

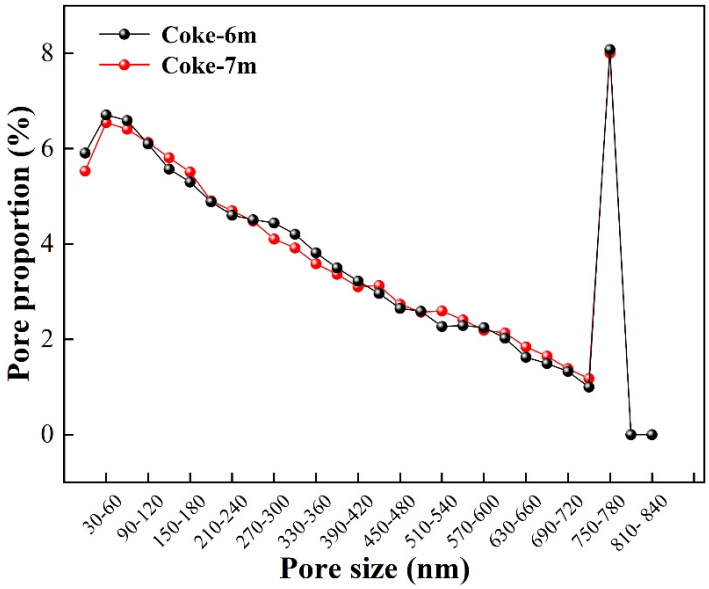


Figure 6. The micro-pore size distribution of coke samples.

In summary, the characterization results of Coke-6m and Coke-7m indicate that the industrial coke oven size has little influence on the micro-pore structure of coke. Some studies have shown that the micro-pore structure has an important impact on coke macroscopic quality [26]. However, as far as the results of this paper are concerned, the contribution of micro-pore structure to the macroscopic quality difference of the two cokes is relatively small.

3.4.2. Nano-Pore Structure

The adsorption and desorption isotherms of the two cokes measured by the low-temperature N_2 adsorption method are shown in Figure 7. The adsorption isotherms of the two cokes are closest to Type II of the International Union of Pure and Applied Chemistry (IUPAC) classification [27]. The results of the two cokes both show that there is an adsorption hysteresis loop between the desorption isotherm and adsorption isotherm, which is similar in shape to Type H_3 in the IUPAC classification [28]. The adsorption hysteresis loop of Coke-7m is significantly larger than that of Coke-6m, indicating that Coke-7m has a more developed nano-pore cavity structure.

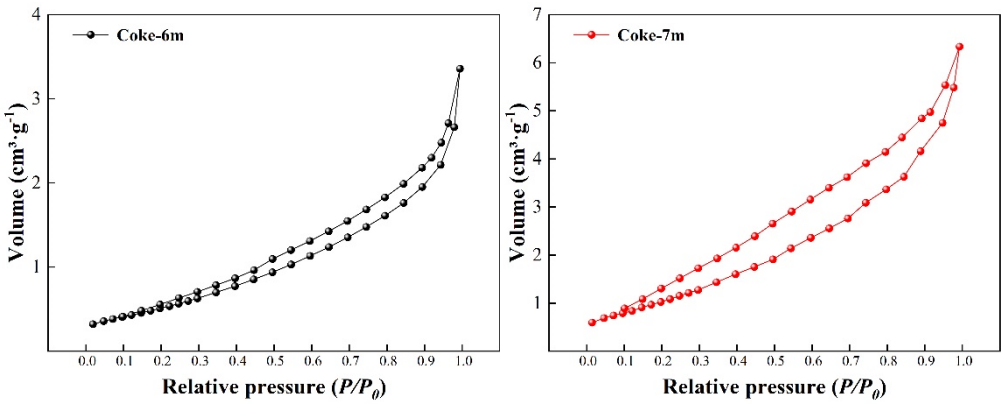


Figure 7. Adsorption and desorption isotherms of coke samples.

According to the adsorption and desorption curves, the nano-pore structure parameters of coke samples can be calculated using methods such as Brunauer–Emmett–Teller (BET), Barrett–Joyner–Halenda (BJH), etc., as shown in Table 12 [29]. The specific surface area S and pore volume V of Coke-7m were obviously larger than those of Coke-6m,

with values about twice those of Coke-6m. The average pore size $\overline{r}$ of Coke-7m was slightly smaller than that of Coke-6m. These results indicate that the nano-pore structure of Coke-7m is more developed, and there are more pores with small pore size.

Table 12. Nano-pore structure parameters of coke samples.

Coke Sample	Specific Surface Area S (m^2/g)	Pore Volume V (mm^3/g)	Average Pore Size $\overline{r}$ (nm)
Coke-6m	2.00	5.20	10.40
Coke-7m	4.13	9.80	9.49

To further explore the differences in the nano-pore structure between the two cokes, the nano-pore size distribution curves of coke samples were plotted, as shown in Figure 8. The pore size distribution curve of Coke-7m was significantly higher than that of Coke-6m, especially for the <10 nm pores. The above phenomenon further indicates that the nano-pores in Coke-7m are more developed, especially with a larger number of small pores with pore size <10 nm.

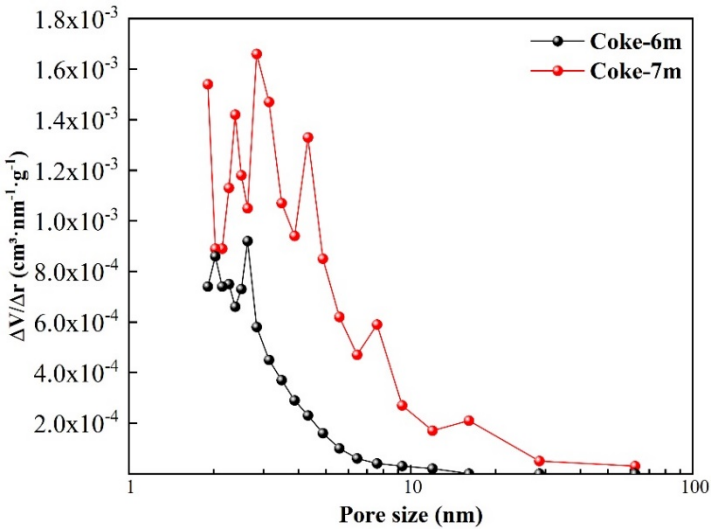


Figure 8. The nano-pore size distribution of coke samples.

Some studies have shown that a more developed nano-pore structure of coke may be unfavorable to its macroscopic quality [17]. However, in this paper, the nano-pore structure of Coke-7m is more developed than that of Coke-6m, but the macroscopic quality of Coke-7m is better than that of Coke-6m. Therefore, it can be seen that the contribution of nano-pore structure to the macroscopic quality difference of the two cokes is very small.

3.5. Discussion

Both Wang et al.'s [17] and Donskoi et al.'s [26] studies found that the pore structure of coke has an important influence on its macroscopic properties. However, based on the comprehensive analysis of the macroscopic and microscopic test results of Coke-6m and Coke-7m, it can be found that different industrial coke oven sizes have little influence on the pore structure of the refined metallurgical cokes. With neither micro-pores nor nano-pores, did large-capacity coke ovens achieve obvious advantages in terms of coke pore structure. But the macroscopic property of Coke-7m is better than that of Coke-6m. This indicates that pore structure is not the only factor affecting the macroscopic property of coke. The carbon structure may have a more important influence on the macroscopic property of coke.

The results obtained by Fujita et al. [23] and Zheng et al. [25] showed that the carbon structure of coke has an important influence on its macroscopic properties. The results of this paper showed that different industrial coke oven sizes have significant influence on the

carbon structure of the refined metallurgical cokes. The optical texture test results showed that the coarse mosaic texture and fibrous texture contents of Coke-7m was obviously higher than those of Coke-6m. The microcrystalline structure test results showed that the microcrystalline size of Coke-7m was larger than that of Coke-6m, and the microcrystalline structure of Coke-7m was denser. Therefore, both the optical texture and microcrystalline structure indicate that the carbon structure of Coke-7m is superior to that of Coke-6m. It can be inferred that the metallurgical coke refined by large-capacity coke ovens has obvious advantages in carbon structure.

The advantages of Coke-7m in terms of carbon structure may be an important reason for its superior macroscopic quality compared to Coke-6m. From the macroscopic quality indexes, the chemical compositions of the two cokes are similar, which may be related to the use of the same raw coals and proportions. The conventional cold and thermal property indexes (M_{40}/M_{10}, CRI/CSR) of Coke-7m are superior to those of Coke-6m, indicating that its macroscopic quality is better. The coke thermal strengths (CSR25s) at multiple temperatures further indicate that, at low or high temperatures, when the coke solution-loss reaction mode tends to be the "uniform reaction model" or "unreacted core model", the thermal strengths of Coke-7m are higher than those of Coke-6m. At medium temperatures, when the coke solution-loss reaction mode tends to be the "gradient reaction model", the thermal strengths of the two cokes are close. When the coke sample is in the "gradient reaction model", the damage effect on its thermal strength is greater, and the advantages in carbon structure of Coke-7m may be offset by the unfavorable influence of its nano-pore structure. Therefore, the thermal strengths of the two cokes are close at this time.

The above results indicate that the large-capacity coke oven has a certain effect on improving the quality of metallurgical coke. In addition, Yin et al. [30] pointed out that the coking industry is a combination of discrete and continuous production processes. Increasing the effective capacity of coke ovens is conducive to reducing the amount of coke discharging and coal loading under the premise of refining the same output of coke, thus reducing the emission of paroxysmal pollutants. In view of the many benefits of large-capacity coke ovens in improving coke quality, promoting cleaner production, and realizing sustainable development, China and even countries around the world should vigorously develop large-capacity coke ovens.

4. Conclusions

The influence of industrial coke oven size on the quality of metallurgical coke was comprehensively demonstrated from two aspects: macroscopic quality indexes (including conventional quality indexes and thermal strength indexes at multiple temperatures) and microstructure (carbon structure and pore structure). The main conclusions are as follows:

1. The conventional quality indexes show that the cold and thermal strengths of Coke-7m are higher than those of Coke-6m, indicating that the large-capacity coke oven plays a role in improving the quality of metallurgical coke;
2. The thermal strength indexes at multiple temperatures show that the large-capacity coke oven obviously improves the thermal strength when coke solution loss tends to the "uniform reaction model" or "unreacted core model" at low or high temperatures but has little effect on the thermal strength when coke solution loss tends to the "gradient reaction model" at medium temperatures;
3. Regarding carbon structure, the optical texture results show that Coke-7m has a higher content of coarse mosaic texture and fibrous texture; the microcrystalline structure results show that Coke-7m has a larger size and denser microcrystalline structure. The existence of advantages in carbon structure may be an important reason for the better macroscopic quality of metallurgical coke refined by large-capacity coke ovens;
4. The industrial coke oven size has little influence on the pore structure of metallurgical coke. The micro-pore structure of Coke-7m is similar to that of Coke-6m, and the nano-pore structure is even more developed than that of Coke-6m.

Author Contributions: Conceptualization, L.H. and J.Z.; methodology, L.H. and H.C.; validation, L.X. and F.L.; investigation, W.H.; resources, L.H.; data curation, L.H.; writing—original draft preparation, L.H.; writing—review and editing, J.Z. and H.C.; visualization, L.X.; supervision, F.L.; project administration, W.H.; funding acquisition, L.H. All authors have read and agreed to the published version of the manuscript.

Funding: This work was supported by the National Natural Science Foundation of China (No. 52274316), China Postdoctoral Science Foundation (No. 2020M671408), and Key Science and Technology Project of HBIS Group Co., Ltd. (HG2020207).

Data Availability Statement: No new data were created or analyzed in this study.

Acknowledgments: We thank university of science and technology liaoning for the support provided for this research work.

Conflicts of Interest: Author Liangyuan Hao was employed by the company HBIS Group Co., Ltd. Author Huan Cheng was employed by the company Jiangsu Yonggang Group Co., Ltd. The remaining authors declare that the research was conducted in the absence of any commercial or financial relationships that could be construed as a potential conflict of interest. The HBIS Group Co., Ltd. and Jiangsu Yonggang Group Co., Ltd. had no role in the design of the study; in the collection, analyses, or interpretation of data; in the writing of the manuscript, or in the decision to publish the results.

References

1. Mao, C.; Feng, M.; Guo, Y. Energy and exergy analysis for a coke oven gas based CCHP system. *J. Mater. Metall.* **2021**, *20*, 282–289.
2. Gu, H. Analysis on the operation of China's steel industry in 2021. *Metall. Econ. Manag.* **2022**, *3*, 18–21.
3. Cheng, H.; Liang, Y.; Guo, R.; Sun, Z.; Wang, Q.; Xie, Q.; Wang, J. Effects of solution loss degree, reaction temperature, and high temperature heating on the thermal properties of metallurgical cokes. *Fuel* **2021**, *283*, 118936. [CrossRef]
4. Geng, Y.; Guo, R.; Li, Y.; Zhang, X.; Lin, J. Characteristics of coke pore formation and its effect on solution loss degradation. *Metall. Res. Technol.* **2020**, *117*, 112. [CrossRef]
5. Huang, J.; Guo, R.; Wang, Q.; Liu, Z.; Zhang, S.; Sun, J. Coke solution-loss degradation model with non-equimolar diffusion and changing local pore structure. *Fuel* **2019**, *263*, 116694. [CrossRef]
6. Zhan, L.; Li, Q.; Gai, Y.; Hou, J. Comparison and analysis of coke quality between top-charge and stamp-charge cokemaking processes with special coal blending composition. *Fuel Chem. Process.* **2020**, *51*, 11–14.
7. Zhang, J.; Lin, J.; Guo, R.; Hou, C. Effects of microscopic characteristics on postreaction strength of coke. *Int. J. Coal Prep. Util.* **2019**, *42*, 1615–1625. [CrossRef]
8. Klika, Z.; Serenčíšová, J.; Kolomazník, I.; Bartoňová, L.; Baran, P. Prediction of CRI and CSR of cokes by two-step correction models for stamp-charged coals—Statistical analysis. *Fuel* **2020**, *262*, 116623. [CrossRef]
9. Díez, M.; Alvarez, R.; Barriocanal, C. Coal for metallurgical coke production: Predictions of coke quality and future requirements for cokemaking. *Int. J. Coal Geol.* **2002**, *50*, 389–412. [CrossRef]
10. Guo, R.; Sun, Z.; Wang, J.; Liang, Y. High-reactivity coke and blast furnace low-cost operation. *Hebei Metall.* **2016**, *2*, 1–4.
11. Guo, R.; Wang, Q. Relationship between coke properties and solution loss behavior and its influence on post-reaction strength of coke. *Rev. Metall.* **2012**, *109*, 443–452. [CrossRef]
12. Zhang, W.; Shi, T.; Zhang, Q.; Cao, Y.; Qian, H.; Wu, X.; Li, J.; Zhang, Q.; Yang, G.; Yang, J. Coke texture, reactivity and tumbler strength after reaction under simulated blast furnace conditions. *Fuel* **2019**, *251*, 218–223. [CrossRef]
13. Li, K.; Zhang, J.; Barati, M.; Khanna, R.; Liu, Z.; Zhong, J.; Ning, X.; Ren, S.; Yang, T.; Sahajwalla, V. Influence of alkaline (Na, K) vapors on carbon and mineral behavior in blast furnace cokes. *Fuel* **2015**, *145*, 202–213. [CrossRef]
14. Zhang, Z.; Xie, F.; Zheng, Y.; Cheng, H.; Wang, Q. Coke microcrystalline texture and its effect on coke reactivity. *J. Fuel Chem. Technol.* **2018**, *46*, 406–412.
15. Mihashi, M.; Soejima, M.; Asakuma, Y.; Yamamoto, T.; Aoki, H.; Miura, T.; Kato, K.; Itagaki, S. Evaluation of matrix of coke strength by nano-indentation method. *Trans. Iron Steel Inst. Jpn.* **2002**, *88*, 188–194. [CrossRef]
16. Guo, R.; Duan, C.; Sun, Z.; Wang, J.; Sun, X.; Liang, Y. Effect of pore structure and matrix reactivity on coke reactivity and post-reaction strength. *Metall. Res. Technol.* **2017**, *114*, 504. [CrossRef]
17. Wang, J.; Xie, Q.; Sun, Z.; Ji, B.; Liang, Y. Pore structure development of coke during carbon solution loss reaction. *Iron Steel.* **2015**, *50*, 8–13.
18. Liu, H.; Li, F. Road of macro-scale operations technology for China's coke oven. *Fuel Chem. Process.* **2009**, *40*, 1–4.
19. Li, J.; Sun, Z.; Liang, Y. Interaction of vitrinites in similar middle-rank coals during coking process. *Fuel* **2022**, *316*, 123334. [CrossRef]
20. Huang, J.; Guo, R.; Tao, L.; Wang, Q.; Liu, Z.; Zhang, S.; Sun, J. Mass transfer coefficient and effective internal diffusion coefficient for coke solution loss reaction with non-equimolar diffusion. *Fuel* **2020**, *278*, 118225. [CrossRef]

21. Xing, X.; Zhang, G.; Rogers, H.; Zulli, P.; Ostrovski, O. Effects of annealing on microstructure and microstrength of metallurgical coke. *Metall. Mater. Trans. B* **2014**, *45*, 106–112. [CrossRef]
22. Liu, J.; Qiu, Y. Measures to improve the quality of coke. *Chem. Eng. Equip.* **2011**, *1*, 73–74.
23. Fujita, H.; Hijiriyama, M.; Nishida, S. Gasification reactivities of optical textures of metallurgical cokes. *Fuel* **1983**, *62*, 875–879. [CrossRef]
24. Flores, B.; Borrego, A.; Diez, M.; Silva, G.; Zymla, V.; Vilela, A.; Osório, E. How coke optical texture became a relevant tool for understanding coal blending and coke quality. *Fuel Process. Technol.* **2017**, *164*, 13–23. [CrossRef]
25. Zheng, H.; Xu, R.; Zhang, J.; Daghagheleh, O.; Schenk, J.; Li, C.; Wang, W. A comprehensive review of characterization methods for metallurgical coke structures. *Materials* **2022**, *15*, 174. [CrossRef] [PubMed]
26. Donskoi, E.; Poliakov, A.; Mahoney, M.; Scholes, O. Novel optical image analysis coke characterisation and its application to study of the relationships between coke structure, coke strength and parent coal composition. *Fuel* **2017**, *208*, 281–295. [CrossRef]
27. Cai, Y.; Liu, D.; Pan, Z.; Yao, Y.; Li, J.; Qiu, Y. Pore structure and its impact on CH_4 adsorption capacity and flow capability of bituminous and subbituminous coals from Northeast China. *Fuel* **2013**, *103*, 258–268. [CrossRef]
28. Wang, G.; Ju, Y.; Yan, Z.; Li, Q. Pore structure characteristics of coal-bearing shale using fluid invasion methods: A case study in the Huainan−Huaibei Coalfield in China. *Mar. Pet. Geol.* **2015**, *62*, 1–13. [CrossRef]
29. Zhang, H.; Cheng, H.; Yang, Q.; Ling, Y.; Sun, Z.; Xiao, L. Optimization of the experimental conditions and calculation methods for determination of coke nanopores. *Coke Chem.* **2021**, *64*, 562–570. [CrossRef]
30. Yin, W.; Xu, L.; Han, D.; Qian, H.; Zhang, Y. Research and analysis of the development trend of modern coking technology. *Coal Chem. Ind.* **2020**, *48*, 27–32.

Disclaimer/Publisher's Note: The statements, opinions and data contained in all publications are solely those of the individual author(s) and contributor(s) and not of MDPI and/or the editor(s). MDPI and/or the editor(s) disclaim responsibility for any injury to people or property resulting from any ideas, methods, instructions or products referred to in the content.